Noninvasive Short-Wavelength Near-Infrared Spectroscopic Method To Estimate the Crude Lipid Content in the Muscle of Intact Rainbow Trout

M. H. Lee,† A. G. Cavinato,‡,§ D. M. Mayes,‡,§ and B. A. Rasco*,†

Institute for Food Science and Technology, HF-10, and Department of Chemistry, BG-10, University of Washington, Seattle, Washington 98195

Short-wavelength near-infrared (SW-NIR) spectroscopy (700–1100 nm) was used to predict the crude lipid content of intact, whole rainbow trout (weight range 66.5–883 g). The measurements were performed noninvasively and in the diffuse reflectance mode by conveying the light to the intact, whole fish over an optical fiber bundle. The backscattered light was collected by a second fiber bundle, concentric to the first, and focused onto the entrance slit of the monochromator. Two multivariate calibration models, a multiple linear regression (MLR) model and a partial least-squares (PLS) model, were used to correlate chemical with spectral data. The best correlation between the laboratory values and predicted values from spectral measurements of crude lipid content was obtained at a site midway between the dorsal fin and the adipose fin above the lateral line. The PLS cross-validation model using three latent variables yielded a standard error of prediction of cross-validation [SEPCV = 2.27% (w/w), $R = 0.81$]. Comparable results were achieved with a MLR cross-validation model using three wavelengths (934, 957, and 845 nm) [SEPCV = 2.48% (w/w), $R = 0.76$]. These results suggest that either a full spectrum or a discrete wavelength SW-NIR method could be used to predict the crude lipid content of fish muscle in whole trout without scale damage or other injuries to the animal.

INTRODUCTION

The development of near-infrared methods that are applicable to fishery products and aquacultured animals has been limited. The primary disadvantage of conventional techniques of proximate analysis and current near-infrared methods used to analyze the body composition of wild-caught and cultured fish are that a significant number of animals must be sacrificed to obtain a representative sample for analysis. Furthermore, the standard methods of analysis provide only a limited amount of information. For example, from proximate analysis only the amount of the solvent-extractable fat but not its distribution within the tissue can be determined. Recently, spectroscopic methods for the proximate analysis of fish tissue have been reported in the near-infrared (Rasco et al., 1991; Gjerde and Martens, 1987) and by mid-infrared transmission (Darwish et al., 1989). These methods are invasive and, in certain cases, require extensive sample pretreatment prior to analysis.

A major limitation to the use of near-infrared analyses for fish tissue has been the interference of water bands with important spectral features of other analytes (Gjerde and Martens, 1987). To overcome these interferences, investigators lyophilized trout muscle prior to analysis and were able to obtain a high correlation ($R = 0.95$) between laboratory and spectral values for both moisture and crude lipid content. Rasco et al. (1991) used near-infrared reflectance spectroscopy (900–1800 nm) to predict the proximate composition of fresh or frozen samples of rainbow trout muscle tissue; the standard error of prediction (SEP) for crude lipid was 3.1% using partial least-squares (PLS) calibration methods.

Here, short-wavelength near-infrared spectroscopy (SW-NIR; 700–1100 nm) has been examined as an alternate means for obtaining spectral data for lipid content in whole, intact fish. In humans, the body composition can be estimated by SW-NIR spectroscopy (Conway et al., 1984). SW-NIR presents several advantages over conventional near-infrared methods (900–2500 nm): (a) Absorption in this wavelength region arises from the third- and fourth-overtone vibrational (CH, OH, NH) transitions which are characterized by low extinction coefficients which allow the use of long path lengths (1–5 cm). (b) Although this study was performed using a scanning spectrophotometer, the same technology can be implemented with inexpensive hardware based on fiber optic components, conventional filters or monochromators, tungsten lamps, and silicon detectors (Mayes and Callis, 1989). (c) Signal-to-noise ratios on the order of 10 000:1 can be obtained, thus making very subtle changes in the spectra useful for analysis. (d) Good quantitative results can be obtained for highly scattering samples (Cavinato et al., 1990; Phelan et al., 1989). Whole, intact fish samples are highly scattering, and a long path length is required for penetration into the fish muscle through the skin and scales.

One disadvantage of SW-NIR spectroscopy is that spectral features often appear quite overlapped and require the use of sophisticated data analysis techniques such as multiple linear regression (MLR) and partial least-squares (PLS) calibration methods to obtain meaningful correlations. Multiple linear regression is a process that uses discrete wavelengths in a sample spectrum to construct a linear model that correlates to a particular analyte concentration (Beebe and Kowalski, 1987). A "stepwise" method was used in this study. Stepwise MLR first chooses a wavelength value from the spectral matrix (**R**) that best correlates to an analyte concentration (c_k) and forms a linear regression equation

$$\hat{c}_k = b_0 + b_i\mathbf{R}_i \quad (1)$$

where $\hat{c}_k$ is the predicted concentration, b_0 is the zero

* Author to whom correspondence should be addressed.
† Institute for Food Science and Technology.
‡ Department of Chemistry.
§ Present address: D² Development, 1108 J Ave., La Grande, OR 97850.

0021-8561/92/1440-2176$03.00/0

intercept, b_i is the slope, and $\mathbf{R}_i$ is the absorbance value at wavelength i. Successive wavelength values are incorporated into the model by choosing a second wavelength that best correlates to the residuals of $\hat{c}_k - c_k$; yielding a new model

$$\hat{c}_k = b_0 + b_1\mathbf{R}_i + b_2\mathbf{R}_j \quad (2)$$

where $\mathbf{R}_j$ is the second wavelength chosen. This procedure is repeated until additional wavelengths no longer improve the correlation. The advantage of this approach vs other methods is that only a minimal number of wavelengths need be present in the **R** matrix used for calibration. This makes the technique useful for fixed filter instrumentation. Partial least-squares (PLS) is a full-spectrum analysis tool (Haaland and Thomas, 1988; Sharaf et al., 1986). In this calibration method, new sets of basis vectors are calculated which attempt to correlate the maximum variance in the spectral matrix **R** with the variance in the concentration matrix **C**. When information obtained from the concentration matrix is integrated into the calculation of scores and loadings for the spectral data matrix, more relevant information regarding the component of interest is placed in the earlier PLS factors. Thus, a more refined calibration equation is built that is more representative of the variance due to the analyte of interest compared to other full-spectrum techniques such as principal component analysis (PCA).

MATERIALS AND METHODS

Fish Samples. Rainbow trout (*Oncorhynchus mykiss*) ranging in weight from 66.5 to 883 g were provided by the University of Washington School of Fisheries (Seattle, WA), the Northwest Alaskan Fisheries Center (National Marine Fisheries Center, Seattle, WA), and Cranmar Trout Farms (Kent, WA). The trout were killed by a blow to the head. Sacrificed animals were weighed, numbered, wrapped in plastic wrap, and stored at −30 °C. After spectral analysis, each fish was eviscerated and cut into sections. The flesh surrounding the site where the individual spectra were recorded was ground and analyzed for crude lipid content, using the acid hydrolysis method (method 948.15) (AOAC, 1990). The pooled standard deviation for crude lipid on dry weight basis (dwb) was 0.73% for 52 samples analyzed in triplicate [8.6–25.3% lipid on a dry weight basis (dwb)]. Moisture content was determined as previously described (Rasco et al., 1991). Average concentrations determined by the reference method were used for each sample in establishing the calibration model.

Spectroscopy. SW-NIR spectra of whole fish were recorded at three different locations on the dorsolateral surface above the lateral line on the left side of the animal: (1) midway between the posterior end of the opercle and the anterior insertion of the dorsal fin (left behind head); (2) midway between the anterior insertion and the posterior insertion of the dorsal fin (left under dorsal); (3) midway between the posterior insertion of the dorsal fin and the anterior insertion of the adipose fin (left behind dorsal). Spectral readings were taken without removing the skin and scales. Spectra were recorded using a Pacific Scientific 6250 scanning near-infrared spectrophotometer (NIRS, Inc., Silver Spring, MD) equipped with a bifurcated fiber optic probe. The area examined by the fiber optic probe was approximately 1 cm². A tungsten lamp was used as the light source with wavelength selection by means of an oscillating concave holographic grating. A silicon detector was located at a 0° angle to the incident radiation. Before spectra were taken at each site, a reference spectrum was obtained by reflecting the radiation off of a 5 cm diameter ceramic plate. Spectral values obtained from the fish were ratioed to this "reference spectrum" and then linearized to the concentration data using a $\log_{10}$ transformation and yielding a pseudo absorbance A_R

$$A_R = \text{Log}\,(R_0/R) \quad (3)$$

where R_0 is the reference spectrum and R is the light intensity returned to the system from the sample. The wavelength range was limited to 700–1050 nm in these experiments since the signal-to-noise level decreases dramatically beyond 1050 nm due to a loss of sensitivity of the silicon detector. All spectra were the result of averaging 64 scans, taking approximately 30 s.

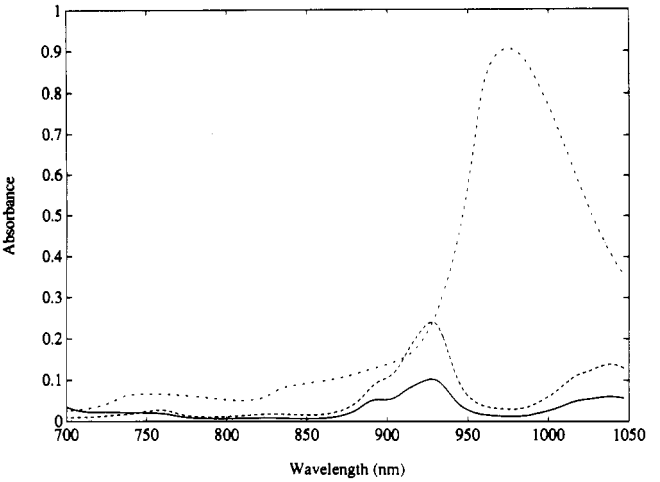

Figure 1. SW-NIR absorbance spectra of pure water (−·−), pure vegetable oil (——), and fish oil (—).

Data Analysis. All data preprocessing and regression computations were performed on a 486 25-Mhz IBM compatible computer with functions developed in MatLab 386 (The MathWorks, Inc., v. 3.5j). Prior to analysis, spectra were smoothed and a second-derivative transformation was calculated using a 16-nm window. In comparing spectra obtained in different experiments, the same smoothing and second-derivative parameters were used. Because of the limited amount of samples, the predictive capabilities of the models generated with both MLR and PLS were tested using a cross-validation routine (Sharaf et al., 1986). This procedure involves a "leave-one-out" approach to multivariate analysis by using the data set minus one sample to develop a calibration model. The model is then used to predict the concentration value for the "left out" sample. Each sample in the sample set is omitted from the calibration model in turn: therefore, if there are n samples in the sample set, the model provides n predicted constituent values which can be compared with the reference method values to determine a standard error of prediction of cross-validation (SEPCV).

RESULTS

Spectroscopic Assignments. The spectra of pure water, pure vegetable oil, and fish oil in the spectral region 700–1050 nm (1 cm path length) are shown in Figure 1. For water the prominent band is at 960 nm. This band arises from the overtone combination band of the OH stretch and bending mode. In addition, weaker absorptions at 840 and 730 nm can also be distinguished. For the vegetable oil and fish oil spectra, the most prominent band is at 930 nm, the third-overtone CH stretch of the methylene group. The band at 893 nm can be assigned to the third overtone of the CH stretch on the methyl group and the weak band at 762 nm to the fourth overtone of the CH stretch on the methylene group (Osborne and Fearn, 1986). The second derivative of a complex spectrum could be used to reduce the effects of baseline offsets due to probe placement in the single-beam spectrophotometer and scattering from the fish scales. It also sharpened spectral features so that broad and overlapping peaks could be better distinguished. The second derivatives were used for comparison of individual peaks since effects due to the overlapping bands were reduced. The second-derivative spectra of pure water, pure vegetable oil, and fish oil are shown in Figure 2.

The spectra of the rainbow trout taken at the site midway between the anterior insertion and the posterior insertion

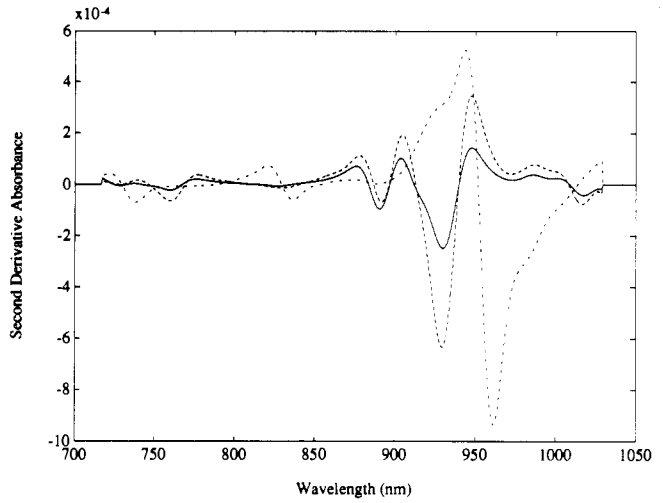

Figure 2. SW-NIR second-derivative absorbance spectra of pure water (- · -), pure vegetable oil (——), and fish oil (—).

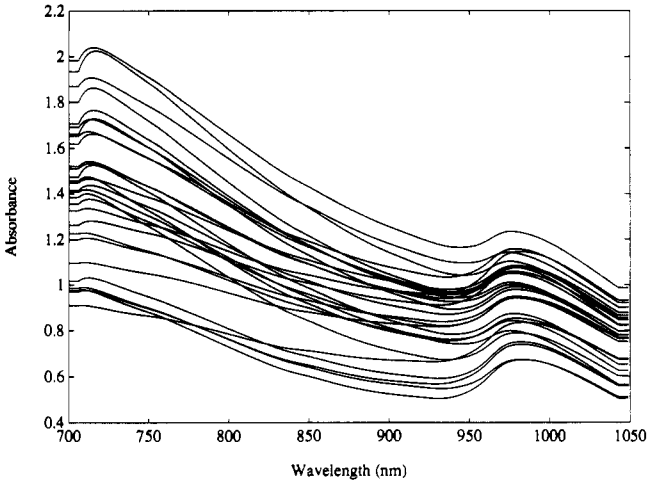

Figure 3. SW-NIR absorbance spectra of rainbow trout recorded at site 2.

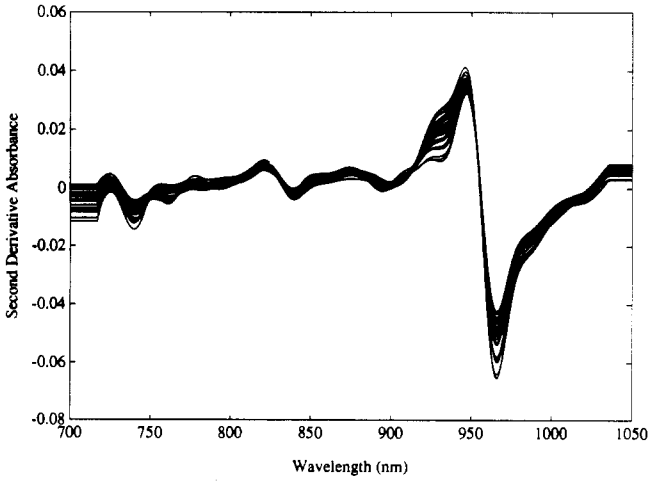

Figure 4. SW-NIR second-derivative absorbance spectra of rainbow trout recorded at site 2.

of the dorsal fin above the lateral line (site 2) are shown in Figure 3. The second derivative of the same set of spectra in Figure 3 are shown in Figure 4. For lipid, the prominent band was at 934 nm and was assigned to the third-overtone CH stretch on the methylene group. The band at 893 nm was due to the third overtone of the CH stretch of the methyl group, and the weak band at 845 nm was assumed to be the 840-nm peak from the pure water

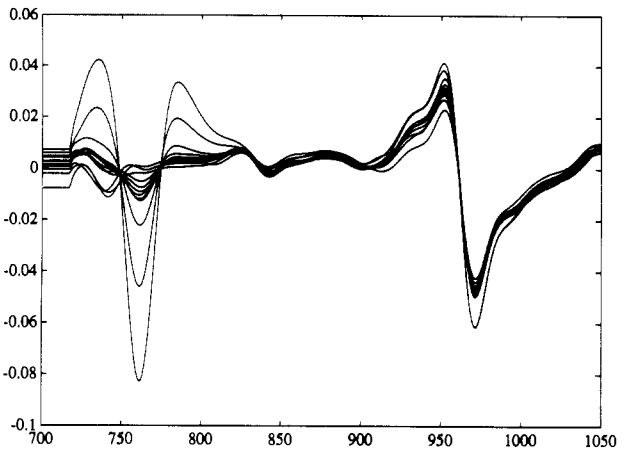

Figure 5. SW-NIR second-derivative absorbance spectra of rainbow trout recorded at site 1.

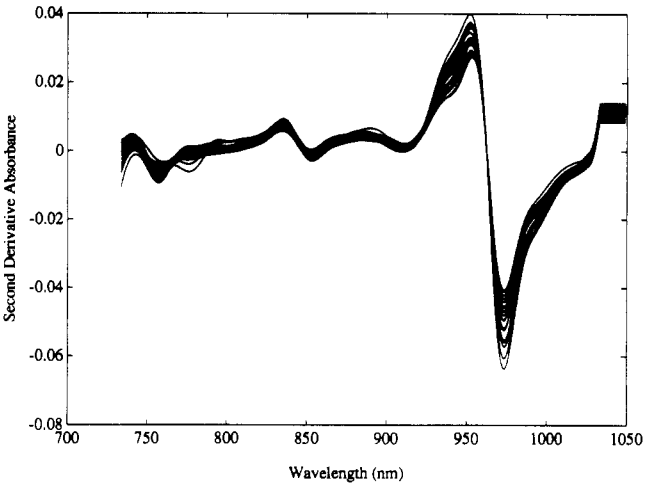

Figure 6. SW-NIR second-derivative absorbance spectra of rainbow trout recorded at site 3.

spectrum (Figure 1). The other weak band at 762 nm was assigned to the fourth overtone of the CH stretch on the methylene group, while the band at 750 nm is an electronic transition from deoxyhemoglobin (Eaton and Hofrichter, 1981). The prominent band at 960 nm arises from the overtone combination band of the OH in water. Changes in the methylene band at 934 nm due to differences in lipid concentration were distinct.

Similar spectral features were observed in the second-derivative spectra taken at the site midway between the gill (posterior end of the opercle) and the anterior insertion of the dorsal fin above the lateral line (site 1) and at the site midway between the posterior insertion of the dorsal fin and the anterior insertion of the adipose fin above the lateral line (site 3) (Figures 5 and 6). At site 1 a more pronounced peak around 750 nm results from the presence of deoxyhemoglobin (Figure 5), as expected, since this spectral site was near the gills. In contrast, sites 2 and 3 exhibit a much lower deoxyhemoglobin content. The second-derivative spectra recorded at sites 1–3 were analyzed by cross-validation MLR and cross-validation PLS to determine the best correlation between spectral and lipid values by acid hydrolysis and the best probe placement for lipid measurement.

Correlation of Lipid with SW-NIR Spectra by MLR. The mean, standard deviation, and range of lipid content at the three different sites in the calibration set are presented in Table I. Stepwise multilinear regression with cross-validation was performed on the second-derivative SW-NIR spectra recorded at sites 1–3, respectively. Table

Table I. Statistics of Lipid Content in the Calibration Set (Dry Weight Basis)

site[a]	mean, %	STD, %	range, %
1	23.2	7.5	5.8–37.7
2	16.0	4.4	6.9–28.1
3	14.1	3.9	5.3–23.7

[a] Spectra taken at three locations on the dorsolateral surface above the lateral line on the left side of the animal: site 1, midway between posterior end of the opercle and the anterior insertion of the dorsal fin (left behind head); site 2, midway between the anterior insertion and posterior insertion of the dorsal fin (left under dorsal); site 3, midway between the posterior insertion of the dorsal fin and anterior insertion of the adipose fin (left behind dorsal).

Table II. Prediction Results for MLR Method and Regression Wavelengths Selected

site[a]	1st, nm	2nd, nm	3rd, nm	R^2	SEPCV,[b] %
1	871			0.53	6.27
2	934			0.64	3.12
	934	957		0.66	3.09
	934	957	1020	0.67	3.08
3	934			0.63	2.96
	934	957		0.69	2.74
	934	957	845	0.76	2.48

[a] Spectra taken at three locations on the dorsolateral surface above the lateral line on the left side of the animal: site 1, midway between posterior end of the opercle and the anterior insertion of the dorsal fin (left behind head); site 2, midway between the anterior insertion and posterior insertion of the dorsal fin (left under dorsal); site 3, midway between the posterior insertion of the dorsal fin and anterior insertion of the adipose fin (left behind dorsal). [a] SEPCV, standard error of prediction of cross-validation.

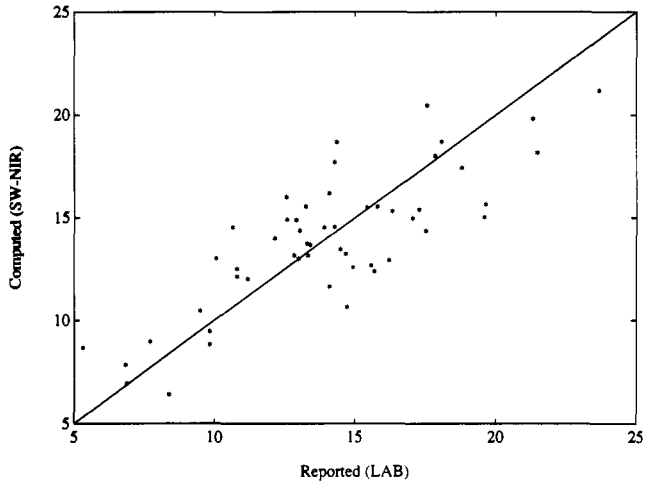

Figure 7. Correlation plot of actual vs three-wavelength regression predicted percent lipid in rainbow trout from second-derivative SW-NIR spectra recorded at site 3.

II summarizes the results of the analysis. Using the correlation coefficient value as a measure of the extent of correlation, it can be seen that site 3 appears to be the best suited for lipid content analysis. The proper number of wavelengths to retain was determined by examining the predicted residual error sum of squares (PRESS) (Sharaf et al., 1986) of the MLR model as a function of wavelengths retained. The PRESS results were obtained from the cross-validation analysis of the second-derivative SW-NIR spectral data. The minimum standard error of prediction occurs with a three-wavelength model. This model yielded a correlation coefficient of 0.76 and a standard error of prediction from cross-validation (SEPCV) of 2.48%. Figure 7 is a correlation plot of the lipid content by acid hydrolysis vs the predicted values for lipid from the three-wavelength regression equation utilizing the second-derivative SW-NIR spectra. These three-wavelength terms can be tentatively assigned to lipid (934 nm) and moisture (957 and 845 nm) absorbances. The introduction in the model of two wavelengths associated with water improves the linearity of the system as shown by an increase in the correlation coefficient value from 0.63 in the one-wavelength model to 0.76 in the three-wavelength model. This was probably due to concomitant changes in the water content in the fish; as moisture content increases, lipid content decreases. In contrast, no significant improvement in the prediction ability of the model was observed at site 2 when a third wavelength was introduced, where the stepwise routine chose 1020 nm which could tentatively be assigned to protein. It is possible that minor interferences from protein present at site 2 compared to site 3 were due to spectral properties of the air bladder and possibly visceral matter, particularly for the smaller fish. The very poor correlation observed at site 1 may be due to the presence of the large deoxyhemoglobin peak, the high concentration of vascular tissue near the head of the fish, and the proximity of this site to the dorsal sinus.

Table III. Prediction Results for PLS Method

site[a]	LV[b]	R^2	SEPCV,[c]
1	4	0.54	6.64
2	4	0.66	3.12
3	3	0.81	2.27

[a] Spectra taken at three locations on the dorsolateral surface above the lateral line on the left side of the animal: site 1, midway between posterior end of the opercle and the anterior insertion of the dorsal fin (left behind head); site 2, midway between the anterior insertion and posterior insertion of the dorsal fin (left under dorsal); site 3, midway between the posterior insertion of the dorsal fin and anterior insertion of the adipose fin (left behind dorsal). [a] LV, latent variables. [c] SEPCV, standard error of prediction of cross-validation.

A useful way to visualize the relationship between wavelength and chemical properties is to examine the variation in correlation (R value) over the spectral region. Negative correlations were observed with the third overtone of the methyl C–H at 900 nm and the methylene C–H at 934 nm as well as with the water absorption at 845 nm in a plot of correlation coefficient vs wavelength for site 3 (data not given). This analysis confirmed that the statistical technique utilized wavelengths which were consistent with the chemical structure and ignored other spectral information.

Correlation of Lipid with SW-NIR Spectra by PLS. To investigate the potential of a full-spectrum analysis method in predicting lipid content in whole trout, the same data sets were analyzed according to the method of partial least-squares. Both the MLR and PLS analyses gave similar results. Table III gives a summary of the statistical correlations obtained by PLS analysis. These results confirm that site 3 was the one best suited for lipid content analysis for this set of experiments. As in the MLR analysis, the proper number of latent variables to include in the model was determined by examining the PRESS results as a function of the number of independent variables retained. The minimum standard error of prediction was observed with three latent variables. PLS correlations using these results yielded a correlation coefficient of 0.81 and a standard error of prediction from cross-validation (SEPCV) of 2.27%. An analysis of the PLS X-block loadings or spectral vectors related to each latent variable provides a sense of the spectral components associated with the analysis of crude lipid in the samples. PLS X-block loading for the first latent variable at site 3 was similar to the average second-derivative spectrum of the data set. The X-block loadings for the second and

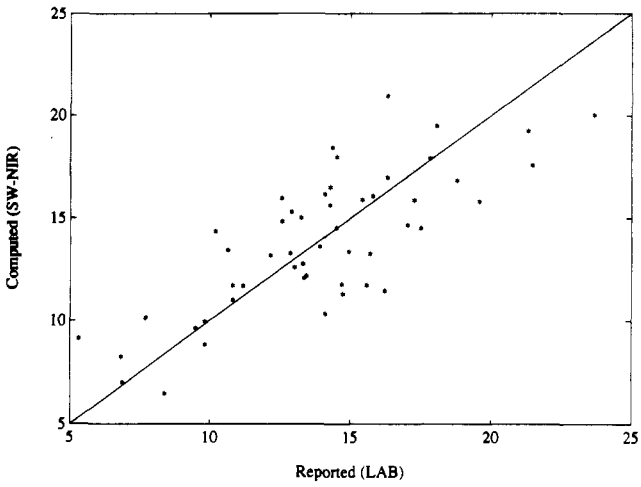

Figure 8. Correlation plot of actual vs PLS predicted percent lipid in rainbow trout from second-derivative SW-NIR spectra recorded at site 3.

third latent variables were quite similar to the MLR correlation spectrum, with the second latent variable giving negative correlations to methyl and methylene absorbances; the third latent variable, while still carrying information associated with the methylene C–H of the lipid, also showed positive and negative correlations to water. Again using multivariate analysis, in this case PLS, appropriate spectral features were selected on the basis of what would be expected given the chemical composition of the sample.

Figure 8 is a correlation plot of the lipid content at site 3 determined by acid hydrolysis vs PLS predicted values. As in the case of the MLR analysis, the prediction errors for lipid were significantly higher than the estimated errors of the laboratory (wet chemical) measurements. However, when examining the individual predictive values, one finds that the extremes in the data set were the principal contributors to the SEP. This suggests that a larger calibration set would improve the precision of the method.

DISCUSSION

Short-wavelength near-infrared spectroscopy would provide measurements of crude lipid content in the muscle of rainbow trout noninvasively without removal of the scales or other injuries to the animal. This analysis was based upon the use of multivariate statistics to find wavelengths or spectral regions that would correlate with the crude lipid content as determined by acid hydrolysis. It was shown that the wavelengths selected statistically were consistent with known absorbance features of the chemical components present in muscle tissue. Although the standard error of prediction as determined by either multiple linear regression (MLR) or partial least-squares (PLS) was significantly higher than the inherent error associated with the reference method, the SW-NIR method could be employed in grading programs or for quality monitoring programs where only approximate values for crude lipid are needed but where rapid analysis or use of a noninvasive method would be important features. The availability of an analytical method such as this could provide the basis for a grading program for salmonids (i.e., segregation based on fat content) and in hatcheries where correlations between body composition and feed conversion could be established without sacrificing stock. Measurement of the body composition of broodstock is also an indication of fecundity and overall health of the animal. As these animals are the group selected for breeding programs based on other criteria, they cannot be sacrificed prior to spawning and their reproductive status must be established by other means, some of which are not precise.

The strength of the SW-NIR method is in its speed and ease. An estimate for a sample can be made in less than a minute and with no sample preparation. In addition, the method can be adapted for field and on-line measurements through the use of inexpensive filter spectrometers. Comparison of MLR and PLS calibrations shows that a discrete model based on three wavelengths has predictive capabilities comparable to those of a full-spectrum analysis. The fact that this noninvasive SW-NIR method provides estimates that are better than those reported previously for an invasive near-infrared method for thin slabs of fresh or frozen rainbow trout muscle (3.1% for lipid) (Rasco et al., 1991) means that long sample path lengths and, if necessary, inexpensive fiber optics can be utilized.

The high prediction errors currently associated with these analyses arise from a number of sources. Although fish scales are highly scattering material, insufficient light may have reached the detector to ensure a high signal-to-noise ratio during spectral acquisition. The use of a single-beam scanning spectrophotometer may have also introduced a high degree of instability due to the irreproducibility in the wavelength selection and placement of the fiber optic probe.

The low precision can also be attributed to the empirical nature of the reference method used to quantitate lipid and the difficulty in obtaining representative samples for analysis (Gjerde and Martens, 1987; Bjarno, 1982). Earlier research indicates that the variance in the nonhomogeneous distribution of lipid in fish muscle is greater than the variance due to the sampling procedure (Rasco et al., 1991; Mathias et al., 1987).

These considerations suggest that the precision of the method could be improved through the use of a better spectrometer for spectral acquisition and stricter control of the sampling procedure. Ideally, the spectrometer should have no moving parts and an adjustable detector exposure time in order to optimize the signal-to-noise ratio (Mayes and Callis, 1989). Improvements in the near-infrared sampling procedure could be achieved by optimizing the fiber probe design and optimizing the distance between the emitting and collecting fibers. Probe placement would also be a critical factor, particularly for fish weighing less than 100 g. As seen in Table II and Figure 5, a large peak for deoxyhemoglobin was present at site 1, the site midway between the posterior end of the opercle and the anterior insertion of the dorsal fin above the lateral line, due to the proximity of this site to the gills and major blood vessels running from the gills along the spine to the body. Spectral features in this region could also have been affected by kidney tissue, the dorsal sinus, or the air bladder. Initially, we believed that spectra taken at site 2, the site midway between the anterior and posterior insertions of the dorsal fin above the lateral line, would have better correlated with muscle crude lipid content than spectra taken at site 3, the site midway between the posterior insertion of the dorsal fin and the anterior insertion of the adipose fin. However, it was possible that the spectra taken at site 2 may have been affected by the dark muscle tissue near the dorsal fin, which has a higher lipid content, or to the presence of a thicker layer of subdermal fat at this site. In addition, spectral readings taken at site 3 may have led to a more even return of

scattered light to the probe as the spine was closer to the surface for site 3 than for site 2.

In summary, a noninvasive SW-NIR reflectance method was developed to estimate the crude lipid content of the muscle in intact, whole rainbow trout taking spectral measurements directly through the skin and scales. Partial least-squares (PLS) and multiple linear regression (MLR) calibrations produced acceptable prediction results (SEP = 2.4%), similar to those reported for crude lipid analysis in other studies using near-infrared (Rasco et al., 1991; Valdes and Summers, 1986). The method can be developed as a rapid, inexpensive tool for field or on-line use, and experiments are underway to improve the precision of the technique by using a photo diode array spectrophotometer.

ACKNOWLEDGMENT

This research was supported by the Egtvedt Food Research Fund, the Cooperative State Research Service, the U.S. Department of Agriculture (Western Regional Aquaculture Consortium, Agreement 87-CSRS-2-3219), and the Center for Process Analytical Chemistry, University of Washington. We thank Zhihong Ge for assistance with portions of the data analysis.

LITERATURE CITED

AOAC. *Official Methods of Analysis*, 15th ed.; Helrich, K., Ed.; Association of Official Analytical Chemists: Arlington, VA, 1984.

Beebe, K. R.; Kowalski, B. R. An Introduction to Multivariate Calibration and Analysis. *Anal. Chem.* **1987**, *59*, 1007A–1017A.

Bjarno, O. C. Multicomponent Analysis of Meat Products. *J. Assoc. Off. Anal. Chem.* **1982**, *65*, 696–700.

Cavinato, A. G.; Mayes, D. M.; Ge, Z.; Callis, J. B. Noninvasive Method for Monitoring Ethanol in Fermentation Processes Using Fiber-Optic Near-Infrared Spectroscopy. *Anal. Chem.* **1990**, *62*, 1977–1982.

Conway, J. M.; Norris, K. H.; Bodwell, C. E. A New Approach for the Estimation of Body Composition: Infrared Interactance. *Am. J. Clin. Nutr.* **1984**, *40*, 1123–1130.

Darwish, G. S.; Van de Voort, F. R.; Smith, J. P. Proximate Analysis of Fish Tissue by Mid-Infrared Transmission Spectroscopy. *Can. J. Fish Aquat. Sci.* **1989**, *46*, 644–648.

Eaton, W. A.; Hofrichter, J. *Methods in Enzymology: Section V, Specific Spectroscopic Properties of Hemoglobins*; Antonini, E., Rossi-Bernardi, L., Cheanncone, E., Eds.; Academic Press: New York, 1981; Vol. 76, p 175.

Gjerde, B.; Martens, H. Predicting Carcass Composition of Rainbow Trout by Near-Infrared Reflectance Spectroscopy. *J. Anim. Breed. Genet.* **1987**, *104*, 137–148.

Haaland, D. M.; Thomas, E. V. Partial Least-Squares Methods for Spectral Analyses. 1. Relation to Other Quantitative Calibration Methods and the Extraction of Qualitative Information. *Anal. Chem.* **1988**, *60*, 1193–1202.

Mathias, J. A.; Williams, P. C.; Sobering, D. C. The determination of lipid and protein in freshwater fish using near infrared reflectance spectroscopy. *Aquaculture* **1987**, *61*; 303–311.

Mayes, D. M.; Callis, J. B. A Photodiode-Array-Based Near-Infrared Spectrophotometer for the 600–1100 nm Wavelength Region. *Appl. Spectrosc.* **1989**, *43*, 27–32.

Osborne, B. G.; Fearn, T. *Near Infrared Spectroscopy in Food Analysis*; Longman Scientific and Technical, Wiley: New York, 1986; p 30.

Phelan, M. K.; Barlow, C. H.; Kelly, J. J.; Jinguji, T. M.; Callis, J. B. Measurement of Caustic and Caustic Brine Solutions by Spectroscopic Detection of the Hydroxide Ion in the Near-Infrared Region, 700–1150 nm. *Anal. Chem.* **1989**, *61*, 1419–1424.

Rasco, B. A.; Miller, C. E.; King, T. L. Utilization of NIR Spectroscopy To Estimate the Proximate Composition of Trout Muscle with Minimal Sample Pretreatment. *J. Agric. Food Chem.* **1991**, 39, 67–72.

Sharaf, M. A.; Illman, D. L.; Kowalski, B. R. Chemometrics. *Chemical Analyses: A Series of Monographs on Analytical Chemistry and Its Applications*; Elving, P. S., Winefordner, J. D., Koltroff, I. M., Eds.; Wiley: New York, 1986, Vol. 82.

Valdes, E. V.; Summers, J. D. Determination of crude protein and fat in carcass and breast muscle samples of poultry by near infrared reflectance spectroscopy. *Poult. Sci.* **1986**, *65*, 485–490.

Received for review April 23, 1992. Accepted August 3, 1992.